Rheologica Acta (2024) 63:603–613
https://doi.org/10.1007/s00397-024-01459-7

ORIGINAL CONTRIBUTION

Rheological properties and the intrinsic mechanisms of fly ash/silicon-based shear thickening fluid

Li Sun[1] · Geng Wang[1] · Chunwei Zhang[2] · Tianqi Liang[1]

Received: 7 March 2024 / Revised: 22 May 2024 / Accepted: 22 May 2024 / Published online: 18 June 2024

Abstract

We have found that the unique particle properties of fly ash can be applied to the modification of shear thickening fluid. In this paper, rheological properties and microscopic thickening mechanism of fly ash/silicon-based shear thickening fluid (subsequently abbreviated as FA/SiO_2-STF) are studied. Ultrasonic technology and mechanical stirring method were used to prepare FA/SiO_2-STF with different mass fractions of fly ash, and then rheometer was used to carry out steady-state rheological testing for FA/SiO_2-STF, and 4%FA/SiO_2-STF dynamic rheological test and temperature sensitivity testing, respectively. The thickening mechanism of FA/SiO_2-STF was analyzed by scanning electron microscope. The rheological test results show that the FA/SiO_2-STF with 4% fly ash content exhibits remarkable shear thickening effect. Finally, the relationship between the viscosity and shear rate of FA/SiO_2-STF is numerically described by a mathematical model, which can accurately reflect the viscosity thickening effect.

Keywords Shear thickening fluid · Fly ash · Rheological property · Non-Newtonian fluid · Shear rate

Introduction

Shear thickening fluid (STF) is a suspension system consisting of nanometer or micron particles as the dispersed phase (Jiang and Pu 2020; Son et al. 2020; Sun et al. 2023). The most common STF is prepared by dispersing silica into ethylene glycol (EG) or polyethylene glycol (Li et al. 2017; Prabhu and Singh 2021; Mahesh et al. 2022). When the shear rate reaches a certain threshold, the viscosity of STF will increase nonlinearly with the increase of the shear rate (Sun et al. 2018; Wei et al. 2020; Heinze and Carastan 2020). Due to the high damping properties of STF during thickening, it can find its use in a variety of engineering applications (Shen et al. 2018; Sun et al. 2021b; Wei et al. 2023), such as body armor, shock absorbers, and sports equipment. At present, improving the thickening effect of STF and its composite application has become one of the current research hotspots.

✉ Li Sun
sunli2009@163.com

[1] School of Civil Engineering, Shenyang Jianzhu University, Shenyang 110168, China

[2] Multidisciplinary Center for Infrastructure Engineering, Shenyang University of Technology, Shenyang 110870, China

With the in-depth understanding of shear thickening fluid, the researchers gradually concluded that dispersed phase, admixtures, and external environment are the main factors that affects shear thickening (ST) (Liu et al. 2016; Yu et al. 2018; Sun et al. 2021a). Among them, the dispersed phase is the key factor restricting the shear thickening effect. Changing the dispersing phase, such as volume fraction, particle size, size distribution, shape, and surface chemistry properties, can dramatically influence the rheological properties of STF (Sun et al. 2018; Zheng et al. 2022). Egres and Wagner (2005) studied the influence of particles' shape on the ST properties of STF. They found that shear thickening was more likely to occur when the dispersing phase was composed of anisotropic particles. The suspension of rod-shaped particles was most prone to show shear thickening behavior, followed by plate particles, while the viscosity of spherical particles STF was the smallest. Wu et al. (2020) developed a novel shear thickening fluid (Z-STF) by dispersing zeolite imidazolate framework-8 (ZIF-8) nanoparticles into ethylene glycol (EG). The rheological properties of Z-STF were controlled by changing the morphology of ZIF-8 nanoparticles. Compared with traditional SiO_2-based STF (S-STF), Z-STF shows a superior shear thickening behavior because of the porous nature and polyhedron morphology of the ZIF-8 nanoparticles. Cheng et al. (2021) used styrene/acrylate

copolymer particles as the dispersed phase to prepare STF and conducted steady-state rheological tests for STF. The experimental results show that STF exhibits shear thinning behavior at low shear rate, while the viscosity increases sharply after the critical shear rate is about 10 s^{-1}, and shear thickening behavior occurs.

The study of dense suspensions remains a diverse field of study, and experimental and computational studies must be used in parallel to reveal the microscopic mechanisms behind their volume rheology and fluid mechanics (Lin et al. 2015; Trulsson et al. 2017; Monti and Rosti 2023). Some scholars have summarized the relevant laws through a large number of experiments and put forward some theoretical models to explain the shear thickening phenomenon. Brady and Bossis (1985) proposed the hydrated particle cluster theory and demonstrated through dynamic simulation that the shear thickening phenomenon was caused by the hydrodynamic forces between particles in STF. In recent years, with the advent of high-resolution optical devices, people can observe the process of the movement of microscopic particles through experimental instruments. Cheng et al. (2011) used confocal electron mirrors to observe the particle motion state of spherical silica suspension during shearing, which directly reflected the thickening process of STF. The hydrated particle cluster theory is mainly aimed at the shear thickening fluid with Brownian motion, but the description of thickening phenomenon caused by non-Brownian particles has some limitations. Therefore, some researchers put forward the frictional contact theory. Trulsson et al. (2017) used a numerical simulation method to systematically change the microscopic friction coefficient and viscosity coefficient of particles and explained the three effects of particles on frictionless, frictional sliding and rolling. Mawkhlieng et al. (2021) prepared a multiphase shear thickening solution (STF) containing graphene nanosheets (GNPs). According to SEM images, GNPs has a larger surface area than silica particles, and the former serves as the gathering point. Smaller silica particles travel relatively little distance and can form clusters on GNPs. Gürgen and de Sousa (2020) added very small cork particles (0.5–1.0 mm) to silicon-based shear thickening suspension and performed microscopic analysis of the deformation of each particle during shear thickening. The experimental results show that due to the deformability of cork, cork particles reduce the bearing capacity of suspension. In addition, increased viscosity in the mixture leads to strong particle contact, which causes cork particles to deform due to their softer structure.

Fly ash (FA) is generally micron particles captured in the flue gas after coal combustion, with a diameter range of 1–100 μm. Most of the fly ash particles are spherical, and a few of them melt at high temperature to form honeycombs with rough surface and different shapes (Romagnoli et al. 2014; Kanti et al. 2020; Hu et al. 2023). In addition, fly ash contains alkaline oxides such as potassium oxide and calcium oxide, which can hydrate with alumina to produce gel products such as calcium aluminate hydrate (Shi et al. 2020; Siang Ng et al. 2020). The special morphology of fly ash particles and hydration products with gel properties can greatly change the interface properties of fly ash particles (Nadziri et al. 2018; Gadkar and Subramaniam 2019; Liu et al. 2020). Kim and Jun (2021) used optical technology to study the agglomeration and dispersion of fly ash particles in cement-fly ash suspension. It was found that the nanoscale spherical dispersed fly ash particles could provide a ball bearing effect between the microscopic aggregates, which reduced the viscosity of the cement-fly ash suspension. Ma et al. (2021) studied the fluidity and strength of cement slurry by grinding fly ash and controlling the particle shape of fly ash. According to the electron microscope scanning image and rheological test results of the fly ash particles, the spherical particles in the fly-cement system could improve the fluidity of cement slurry, but the improvement effect was obviously weakened after grinding treatment. There was significant relationship between spherical failure and ball bearing effect and fluidity. The larger the ball ratio, the higher the mobility.

At present, most scholars have only studied the rheological properties of fly ash suspension or its catalytic properties in the chemical field and have not applied the microscopic morphology and particle size of fly ash in the shear thickening fluid. Considering the excellent thermal stability, diverse micro-morphology, and suitable particle size of fly ash, fly ash is expected to be used as a dispersed phase of STF to optimize ST behavior and deepen the understanding of ST behavior and particle structure. Therefore, the study uses the microscopic morphology and particle size of fly ash to prepare FA/SiO_2-STF to explore its rheological properties and thickening mechanism.

Tests and methodologies

Materials

In this experiment, nanoscale silica particles purchased from China Reckitt Chemical Company were used as the dispersing phase, with an average particle size of 12 nm. PEG200 is a stable transparent liquid with hydroxyl value of 510–623 mgKOH/g, purchased from Shandong Yusuo Chemical Technology Co., LTD., China. N-[3-(Trimethoxysilyl) propyl]ethylenediamine (C8H22N2O3Si), purchased from Shanghai Aladdin Reagent Co., LTD., was used as the dispersant. The fly ash (FA) purchased from Gongyi Yuanheng Water Purification Material Factory was selected as the second dispersed phase, with an average particle size of 6.5 μm. Figure 1 shows the particle size distribution and particle morphology of fly ash.

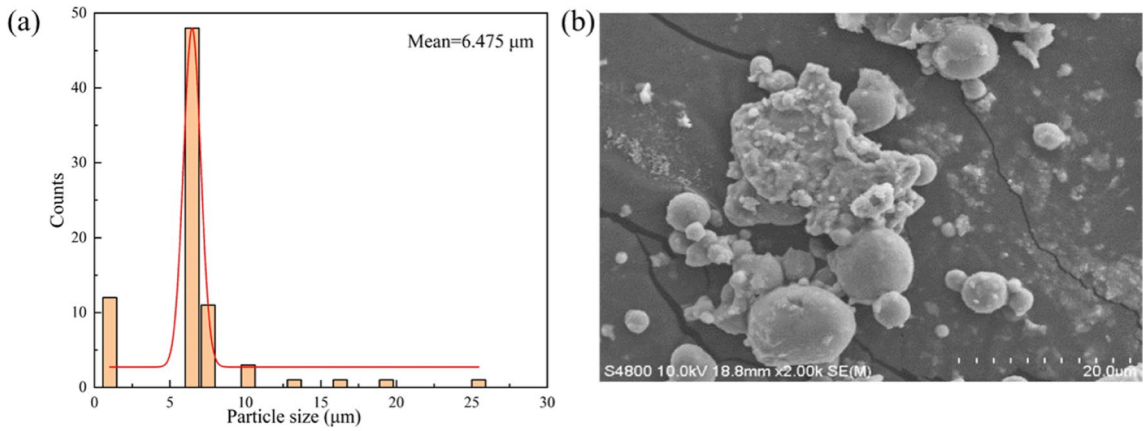

Fig. 1 Physical characteristics of fly ash. **a** Particle size distribution; **b** particle morphology

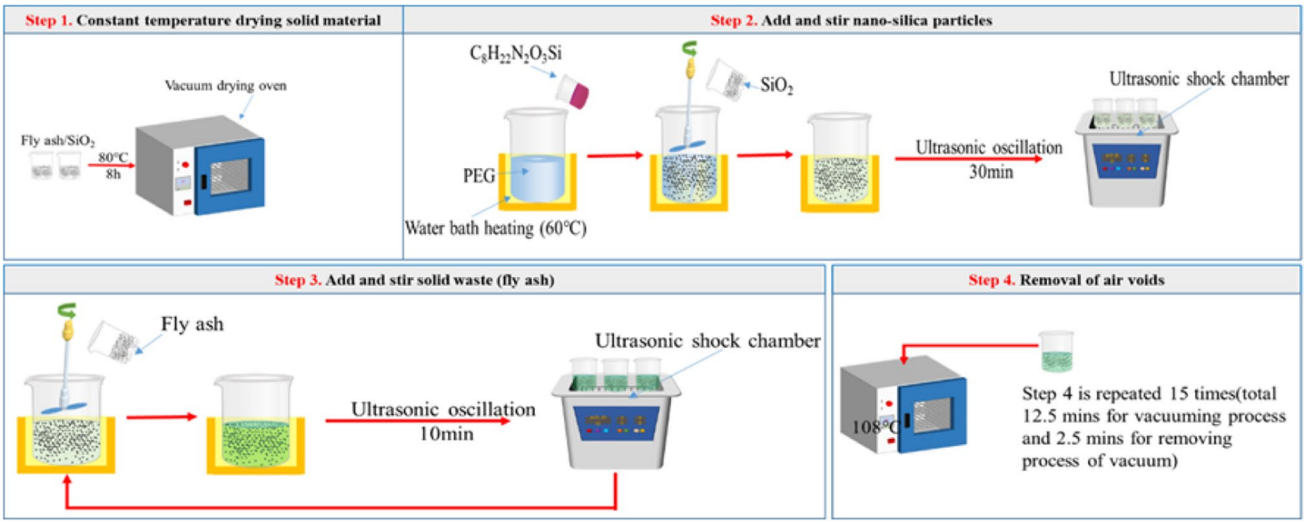

Fig. 2 STF preparation process

STF preparation

The preparation process (Zheng et al. 2020; Wilms et al. 2022; Guo et al. 2023) of STF is shown in Fig. 2. First, before preparing FA/SiO_2-STF, nano-silica particles and fly ash particles were dried in a vacuum drying oven for 8 h. During the preparation process, the constant temperature water bath environment was maintained at 60 °C. A total of 6 STFs were prepared in this work, and the main components of STF sample are shown in Table 1.

First, add 200 ml PEG200 and appropriate amount of C8H22N2O3Si to the beaker. Secondly, during the stirring process, nano-silica is added to the beaker in a pre-set proportion, and the beaker is continuously oscillated for 30 min using an ultrasonic oscillator until the nanoparticles are uniformly dispersed in PEG200. Then, fly ash was added in the same way, and the ultrasonic

Table 1 Main components of STF sample

Sample	PEG (ml)	Nano-silica (g)	Fly ash (g)	C8H22N2O3Si (g)
SiO_2-STF	200.0	50.0	/	2.0
1%FA/SiO_2-STF	200.0	50.0	0.5	2.0
2%FA/SiO_2-STF	200.0	50.0	1.0	2.0
3%FA/SiO_2-STF	200.0	50.0	1.5	2.0
4%FA/SiO_2-STF	200.0	50.0	2.0	2.0
5%FA/SiO_2-STF	200.0	50.0	2.5	2.0

oscillation time was 10 min. Finally, the configured FA/SiO_2-STF was placed in a vacuum drying oven at 108 °C for curing for 2 weeks to obtain stable FA/SiO_2-STF.

Rheological performance test

For each group of materials (about 200 ml, Fig. 3b shows the FA/SiO_2-STF of some samples), 3 locations were randomly selected in the corresponding beakers for sampling. Each sample material was about 5 ml. TA Company AR2000 rheometer was used to test the steady-state and dynamic flow performance of FA/SiO_2-STF with different mix ratios. The plate for rheological testing is 40 mm in diameter. The pre-shearing time is 5 s and the shearing rate is 10 s^{-1}. Each experiment was repeated 3 times. Figure 3 shows the rheometer and sample. Specific tests are as follows:

(1) The test temperature was set at 25 °C and the plate spacing was fixed at 0.5 mm. The shear rate scanning range was 0.1–1000 s^{-1}. The steady-state rheological test of shear thickening fluid with different fly ash content was carried out.
(2) The test angular frequency was fixed at 10 rad/s, and the dynamic rheological test of 4%FA/SiO_2-STF was carried out with the strain scanning range of 0.1–2000%. The test strain amplitude was fixed at 75%, 150%, 300%, and 600% and the frequency sweep range was set at 0.1–600 rad/s. The dynamic rheological test of 4%FA/SiO_2-STF was carried out.
(3) The test conditions were shear rate scanning range of 0.1–1000 s^{-1} and plate spacing of 1 mm. The temperature sensitivity of 4%FA/SiO_2-STF and SiO_2-STF was tested at 5 °C, 12.5 °C, 25 °C, and 40 °C.

Results and analysis

Steady-state rheological property

Figure 4a illustrates the viscosity vs. shear rate curves of FA/SiO_2-STF with different mass fraction ratios in the shear rate scanning range of 0.1–1000 s^{-1}. The plate spacing and temperature are 0.5 mm and 25 °C, respectively. As shown in Fig. 4a, FA/SiO_2-STF has a good shear thickening effect. Compared to SiO_2-STF, the peak viscosity of FA/SiO_2-STF is higher, and the critical shear rate significantly decreases when thickening occurs. When the shear rate increases, SiO_2-STF and FA/SiO_2-STF exhibit three rheological behaviors in sequence, including near-Newtonian behavior, shear thickening behavior, and shear thinning behavior.

As shown in Fig. 4a, fly ash mass fraction and shear rate have a significant impact on the rheological performance of FA/SiO_2-STF. The reason is that the microstructure of fly ash particles is mainly divided into spherical and honeycomb shapes. Among them, there are a large number of spherical particles with varying volume sizes, while there are fewer honeycomb particles with complex spatial structures. At low shear rate, the initial viscosity of SiO_2-STF is greater than that of FA/SiO_2-STF. This is because both nano-silica and spherical fly ash particles can play the role of ball bearing between the honeycomb micro-aggregate. Among them, the ball bearing effect between nano-silica is weak, so the initial viscosity of SiO_2-STF is large. The strong bearing effect of nano-silica on ball fly ash leads to smaller and more stable initial viscosity of FA/SiO_2-STF. As the shear rate continues to increase, the collision between particles inside FA/SiO_2-STF is further intensified, and the ball bearing effect is weakened. This is conducive to the collision between fly ash particles and nano-silica particles, greatly reducing the slip and rotation between fly ash particles, and forming a friction network along the effective path composed of silica particles, thus improving the thickening effect of FA/SiO_2-STF. Because the amount of fly ash contained in FA/SiO_2-STF is different, the shear thickening effect will increase with the increase of fly ash quality. However, excessive fly ash contains certain alkaline substances, which causes the hydration reaction of fly ash. In addition, the particles in the suspension are not uniform, the shape is complex, the surface electrical density is low, or there is a certain aggregation phenomenon, which will lead to precipitation as shown in Fig. 4c. Compared with 4%FA/SiO_2-STF, 5%FA/SiO_2-STF showed weak shear thickening effect.

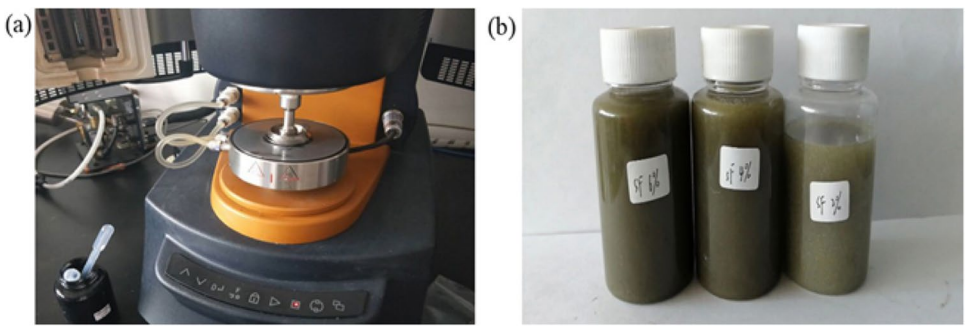

Fig. 3 FA/SiO_2-STF rheological performance testing. **a** Rheometer; **b** partial FA/SiO_2-STF samples

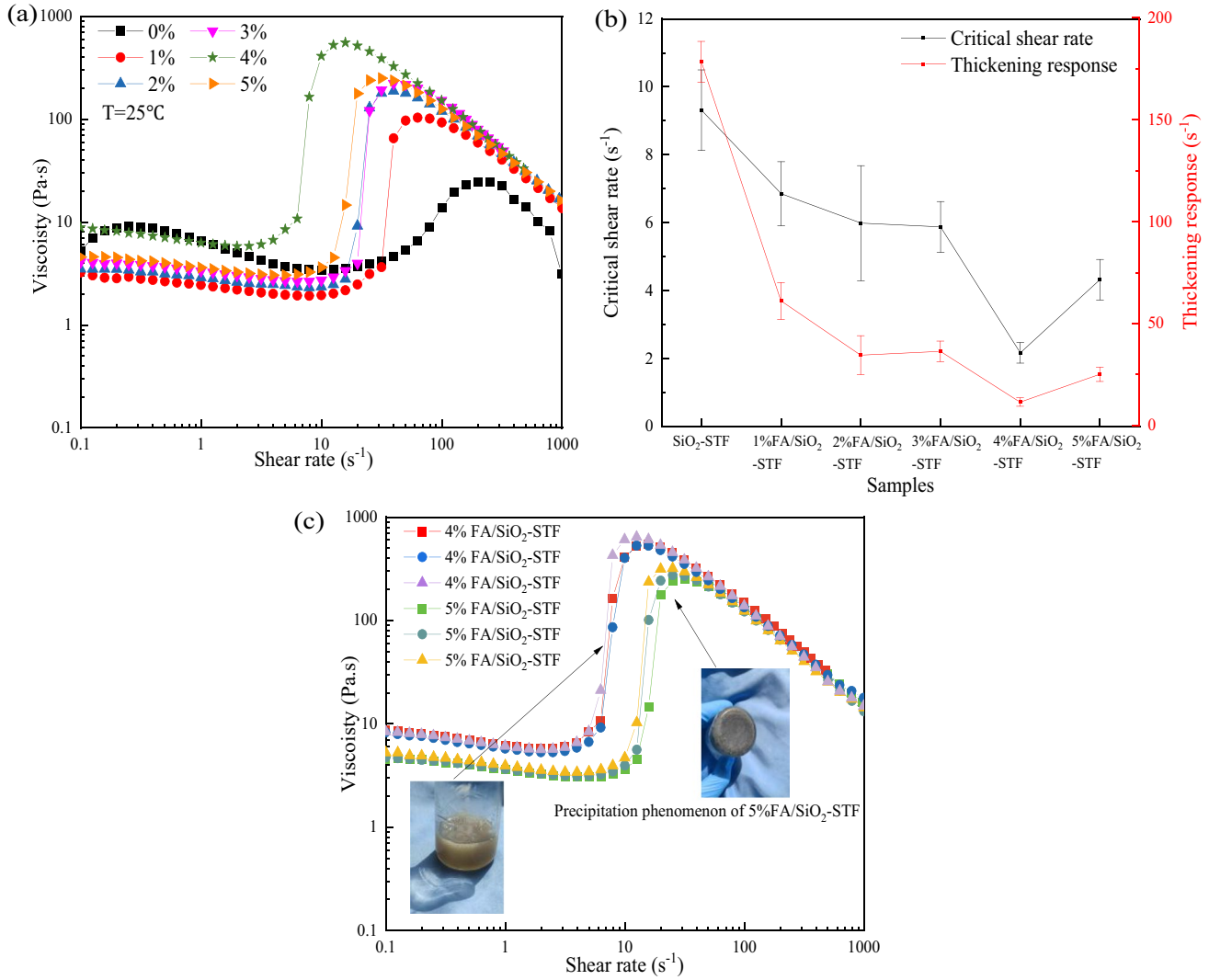

Fig. 4 **a** Rheological properties of FA/SiO_2-STF with different mass fractions of fly ash. **b** Characteristic parameters of FA/SiO_2-STF with different mass fractions of fly ash. **c** Experimental curves and sample images of 4%FA/SiO_2-STF and 5%FA/SiO_2-STF

The critical shear rate is the shear rate corresponding to the minimum viscosity in the thickening process. The difference between the critical shear rate during thickening and the shear rate corresponding to the peak viscosity is the thickening response. As shown in Fig. 4b, with the increase of fly ash mass fraction, the thickening response of FA/SiO_2-STF showed a trend of first decreasing and then increasing. Compared with SiO_2-STF, the critical shear rate and thickening response of FA/SiO_2-STF are significantly reduced. The experimental results show that the particle size and morphology of fly ash can improve the thickening effect of SiO_2-STF. In addition, the variation trend of thickening response also reflects that FA/SiO_2-STF produces thickening behavior mainly through extrusion friction between particles. Most importantly, the thickening effect of 4%FA/SiO_2-STF is significant. As shown in Fig. 4, compared with SiO_2-STF, the peak viscosity of 4%FA/SiO_2-STF increased from 24.65 to 345.02 Pa•s, an increase of 1299.68%, and the thickening response decreased from 189.56 to 22.62 s^{-1}, a decrease of 88.07%.

Temperature sensitive property

In order to further explore the practical application of 4%FA/SiO_2-STF, the influence of ambient temperature on the rheological properties of 4%FA/SiO_2-STF and SiO_2-STF is discussed in detail (Fu et al. 2020; Rizzo et al. 2020; Gürgen and de Sousa 2020). Figure 5a and b show the viscosity-shear rate curves of 4%FA/SiO_2-STF and SiO_2-STF at different temperatures, respectively. As shown in Fig. 5a and b, both 4%FA/SiO_2-STF and SiO_2-STF exhibit obvious shear thinning and shear thickening behaviors at

different temperatures. However, the effect of temperature on shear thickening behavior is significantly greater than its effect on shear thinning behavior. For example, when the temperature increases threefold from 12.5 to 40 °C, the viscosity of 4%FA/SiO_2-STF at a shear rate of 0.1 s^{-1} only decreases by 35.64 Pa•s, while the peak viscosity difference can reach 1987.65 Pa•s.

As can be seen from Fig. 5c and d, compared with SiO_2-STF, 4%FA/SiO_2-STF is greatly affected by temperature. The critical shear rate and thickening response decreased significantly with decreasing temperature. When the temperature of 4%FA/SiO_2-STF decreased from 40 to 25 °C, 12.5 °C, and 5 °C, its thickening response decreased from 23.12 to 14.26 s^{-1}, 3.59 s^{-1}, and 2.35 s^{-1}, respectively. The reduction rates were 38.32%, 84.17%, and 89.84%, respectively. This is because the higher the temperature, the Brownian motion of nano-silica is intensified, which weakens the contact between fly ash particles and other fly ash particles along the effective path composed of silica particles. Therefore, the shear thickening performance of 4%FA/SiO_2-STF will decrease with the increase of temperature.

Microscopic characterization of FA/SiO_2-STF

As shown in Fig. 6, the thickening mechanism of FA/SiO_2-STF was analyzed. The thickening process of STF was studied from two aspects of fly ash particle morphology and contact path. Figure 6a is the image of fly ash particles obtained by scanning electron microscopy (SEM). Fly ash particles have two particle shapes, which are spherical and honeycomb with rough and angular surface. Because of its unique structure and large specific surface area, honeycomb fly ash particles can adsorb a large amount of free nano-silica. Figure 6b is the image of 4%FA/SiO_2-STF particles obtained by scanning electron microscopy (SEM).

Figure 6c describes the shear thickening mechanism of FA/SiO_2-STF. When subjected to shearing action, the

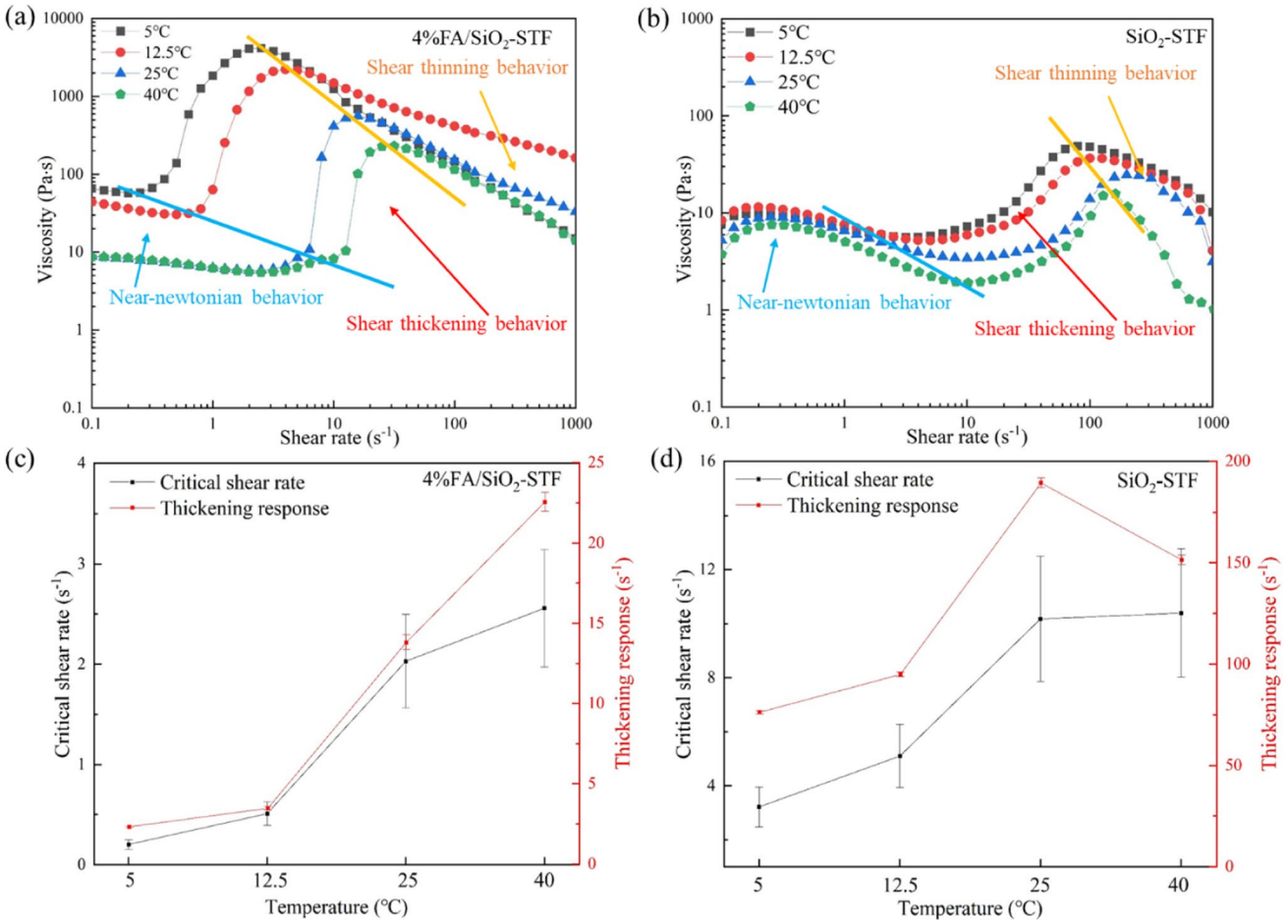

Fig. 5 The rheological properties of STF at different temperatures of **a** 4%FA/SiO_2-STF and **b** SiO_2-STF. The rheological characteristic parameters of STF at different temperatures of **c** 4%FA/SiO_2-STF and **d** SiO_2-STF

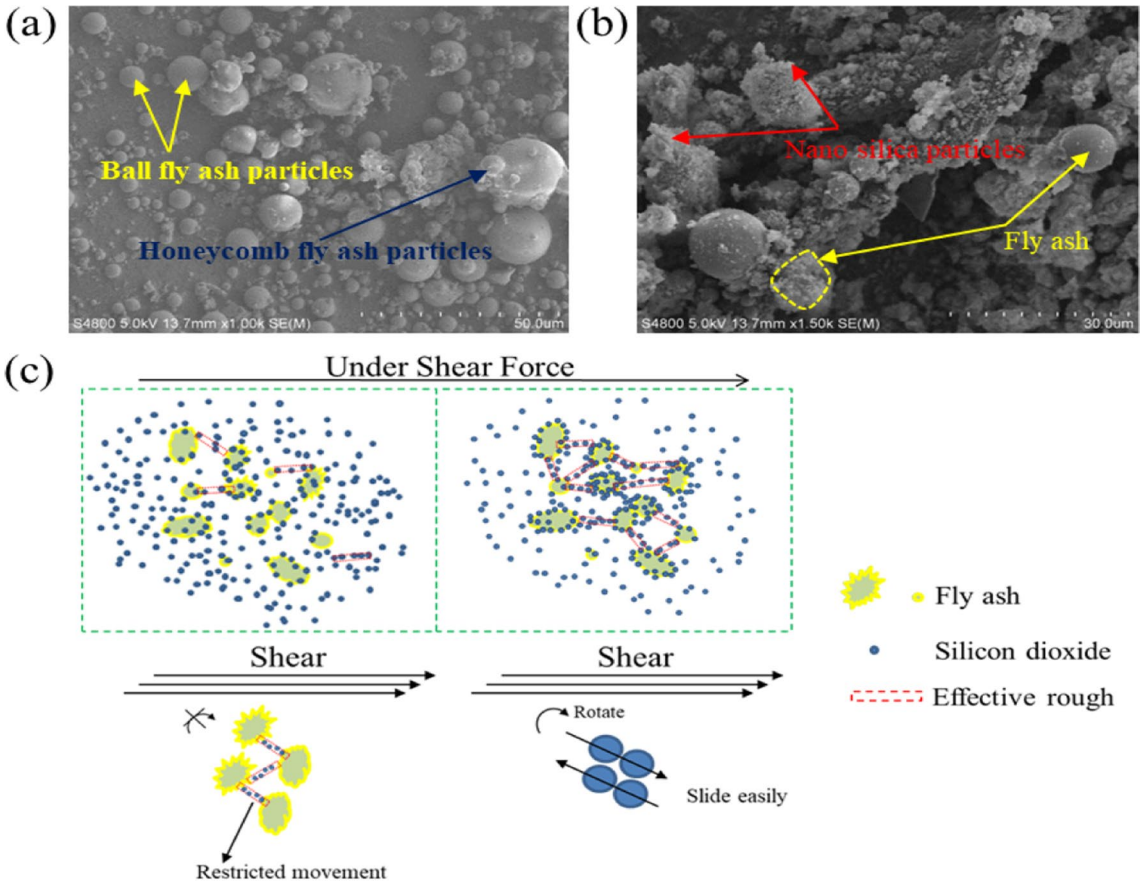

Fig. 6 Microscopic characterization of FA/SiO_2-STF. **a** SEM image of fly ash particles; **b** SEM image of 4%FA/SiO_2-STF particles; **c** thickening mechanism of FA/SiO_2-STF

honeycomb fly ash particles can form particle clusters with a certain amount of nano-silica particles. In addition, as the shear rate continues to increase, the collision between particles in FA/SiO_2-STF is further intensified, and the ball bearing effect generated by nano-silica is weakened. Under shearing action, the chain composed of silica particles can greatly weaken the rotation and slip of fly ash particles, and form a frictional contact network structure, thus improving the thickening effect of FA/SiO_2-STF.

Dynamic rheological property

According to the steady-state rheological experimental results, 4%FA/SiO_2-STF has significant shear thickening performance. Therefore, this section mainly studies the dynamic rheological properties of 4%FA/SiO_2-STF.

Figure 7 shows the curves of the energy storage modulus (G′) and energy dissipation modulus (G″) of 4%FA/SiO_2-STF with the strain amplitude at a fixed angular frequency of 10 rad/s. When the strain amplitude continues to increase, the G′ and G″ curves of 4%FA/SiO_2-STF show a similar trend, starting to increase at about 75% of the strain amplitude, and then weakening when the strain amplitude increases to 600%. The energy storage modulus of 4%FA/SiO_2-STF increases from 34.12 to 837.11 Pa, increasing by

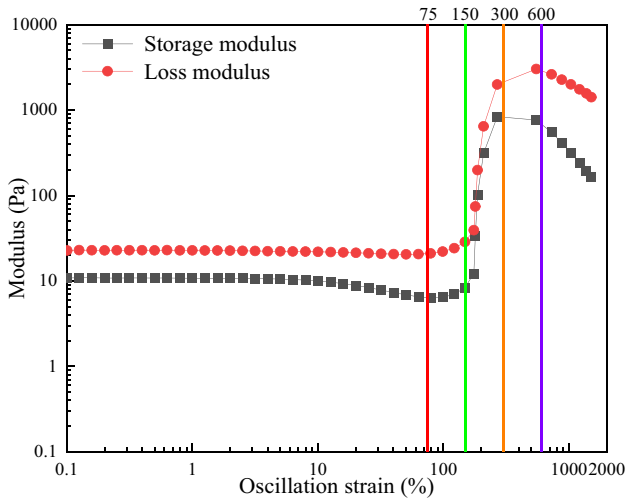

Fig. 7 Relation curve of 4%FA/SiO2-STF modulus and strain amplitude

about 245.34%. The energy dissipation modulus increased from 39.32 to 3024.96 Pa, an increase of about 769.32%. In addition, the energy dissipation modulus of 4%FA/SiO_2-STF is always above the energy storage modulus and is more obvious in the high strain amplitude range, showing stable thickening energy dissipation capacity.

The characteristic strain amplitude points were selected in the 4%FA/SiO_2-STF modulus variation area, and the frequency scanning test was carried out.

Figure 8 shows the curves of the energy storage modulus (G′) and energy dissipation modulus (G″) of 4%FA/SiO_2-STF with the angular frequency under different strain amplitudes. The angular frequency ranges from 0.1 to 200 rad/s. The variation trend of energy storage modulus and energy dissipation modulus of 4%FA/SiO_2-STF is consistent. The modulus of shear thickening fluid increases with increasing angular frequency. With the increase of strain amplitude, the angular frequency corresponding to the significant increase of G′ and G″ of 4%FA/SiO_2-STF decreases. In addition, after the energy dissipation modulus (G″) and energy storage modulus (G′) of 4%FA/SiO_2-STF are significantly increased with the increase of angular frequency, the difference between them increases with the increase of strain amplitude. The energy dissipation capacity of 4%FA/SiO_2-STF is further enhanced and the energy dissipation is obvious at 300% and 600% of strain amplitude. For example, when the strain amplitude is 75% and 300%, the energy dissipation peak of 4%FA/SiO_2-STF increases from 2534.47 to 11,898.70 Pa, an increase of about 369.47%.

Shear thickening fluid viscosity model

The steady-state rheological experiments, dynamic rheological experiments, and temperature sensitivity experiments show that FA/SiO_2-STF has excellent thickening and energy dissipation performance and conforms to the characteristics of non-Newtonian fluids (Qin et al. 2016; Rathee et al. 2020; Thiedeitz et al. 2022; Sun et al. 2024). A mathematical model of the relationship between FA/SiO_2-STF shear rate and viscosity was established, and the fitting results and experimental data are shown in Fig. 9.

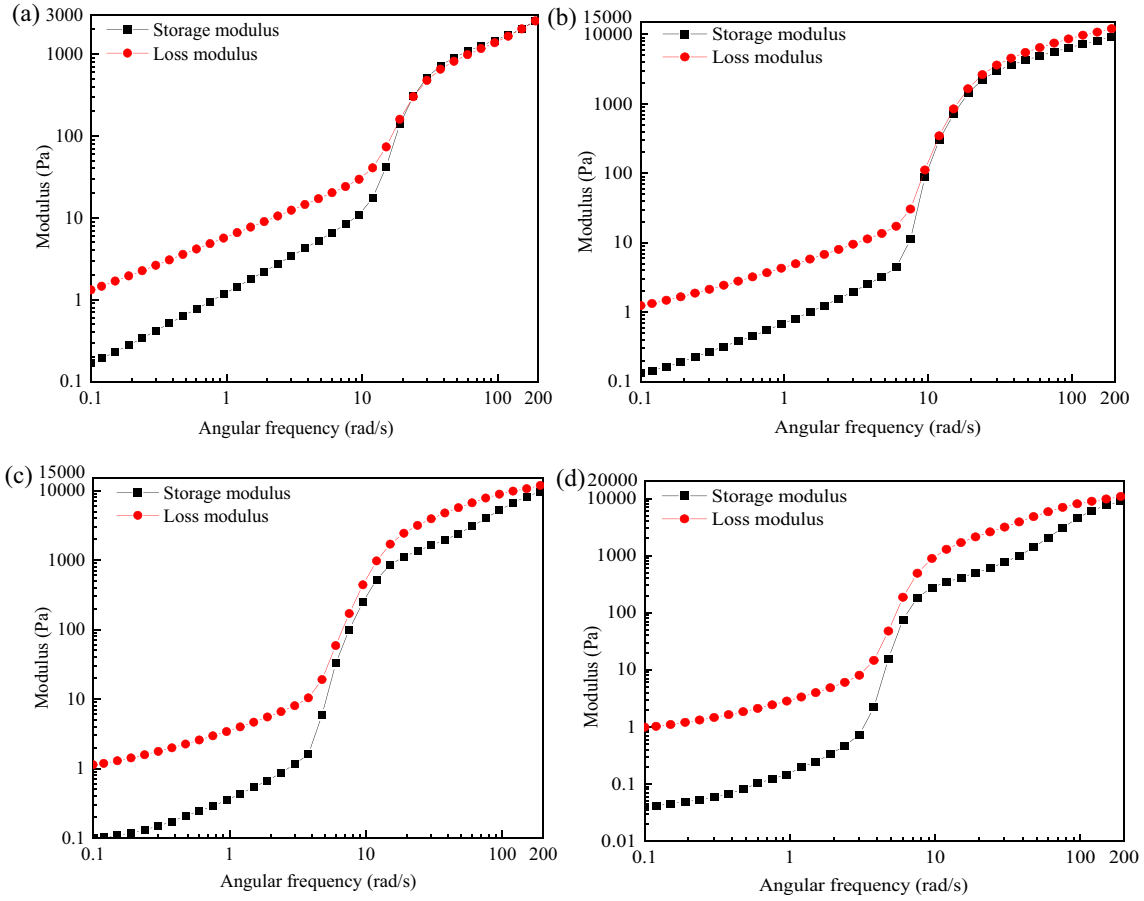

Fig. 8 The relation between the modulus of 4%FA/SiO_2-STF and angular frequency. **a** The strain amplitude is 75%; **b** the strain amplitude is 150%; **c** the strain amplitude is 300%; **d** the strain amplitude is 600%

$$K = \frac{\eta_{max}}{v + T} + \frac{a * (1 - 1/(1 + \exp(b * v + c)))}{1 + \exp(d * v + \dot{\gamma}_c)} \quad (1)$$

K is the apparent viscosity.
η_{max} is the peak viscosity.
T is the constant of temperature.
$\dot{\gamma}_c$ is the critical shear rate.
v is the shear rate.
a, b, c, and d are the adjusting parameters of the curve.

As shown in Fig. 9 that the model can well reflect the viscosity change process of FA/SiO_2-STF and is suitable for the thickening process of FA/SiO_2-STF with different contents. As shown in Table 2, correlation coefficients R^2 of STF viscosity simulation curves with fly ash content of 1%, 2%, 3%, 4%, and 5% are all above 0.95, indicating that the simulation results of viscosity function model have high reliability. The viscosity function model well reflects the two viscosity change stages of FA/SiO_2-STF shear thickening and shear thinning. The empirical formula can provide reference for FA/SiO_2-STF in various engineering applications such as bulletproof vests and shock absorbers.

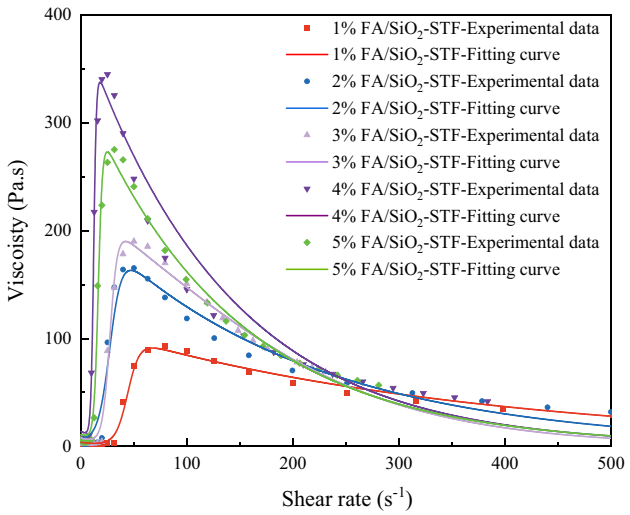

Fig. 9 Comparison between FA/SiO_2-STF experimental data with fitting curves

Conclusion

In this paper, FA/SiO_2-STF with different mix ratios were prepared based on the microscopic morphology of fly ash. Rheological performance of FA/SiO_2-STF was investigated by rheological tests, and the thickening mechanism was revealed based on SEM. Finally, the viscosity changes of FA/SiO_2-STF with different fly ash quality were reflected by mathematical model. The main conclusions are summarized as follows:

(1) 4%FA/SiO_2-STF has shown good shear thickening effect. Fly ash content can greatly affect the ST effect of FA/SiO_2-STF. In addition, the effects of the microscopic morphology of fly ash particles on the shear thickening performance of the fluid are explained by scanning electron microscopy.
(2) Dynamic rheological test shows that 4%FA/SiO_2-STF is an optimal energy dissipation system and can maintain a high energy dissipation effect at lower angular frequency or small strain amplitude. From the point of view of material properties, it shows that the compound has a strong energy dissipation capacity.
(3) The temperature sensitivity test shows that the viscosity of 4%FA/SiO_2-STF is significantly affected by temperatures. The higher the temperature, the more violent the Brownian motion of silica particles, which is not conducive to friction extrusion of fly ash particles along the effective path composed of silica particles.
(4) The viscosity changes of FA/SiO_2-STF in two stages of shear thickening and shear thinning can be accurately reflected by mathematical modeling.

This work makes full use of fly ash particle morphology to improve the ST capacity of FA/SiO_2-STF. The thickening mechanism of FA/SiO_2-STF is analyzed by SEM. The results will greatly assist in the development of intelligent non-Newtonian fluids. However, the physical and chemical properties of the fly ash used in this investigation, such as particle size and calcium oxide content, can only be representative of regional fly ash. In addition, the preparation process, thickening mechanism, and high damping characteristics of FA/SiO_2 in this work can provide insightful reference for researchers in the fields of developing new energy absorption and multifunctional materials.

Table 2 Model parameters and correlation

STF	η_{max}	T	$\dot{\gamma}_c$	a	b	c	d	R^2
1%FA/SiO_2-STF	92.900	25.000	7.943	2,456,000.000	−0.003	−10.010	−0.179	0.988
2%FA/SiO_2-STF	163.918	25.000	5.012	4,777,000.000	−0.005	−10.040	−0.181	0.957
3%FA/SiO_2-STF	190.068	25.000	7.944	345.300	−0.009	0.575	−0.289	0.990
4%FA/SiO_2-STF	345.022	25.000	2.512	5048.000	0.769	−9.332	0.009	0.981
5%FA/SiO_2-STF	275.187	25.000	3.981	17,670.000	0.496	−8.207	0.007	0.989

Data availability Data can be available on request to the authors.

Declarations

Competing interests The authors declare no competing interests.

References

Brady JF, Bossis G (1985) The rheology of concentrated suspensions of spheres in simple shear flow by numerical simulation. J Fluid Mech 155:105. https://doi.org/10.1017/S0022112085001732

Cheng X, McCoy JH, Israelachvili JN, Cohen I (2011) Imaging the microscopic structure of shear thinning and thickening colloidal suspensions. Science 333:1276–1279. https://doi.org/10.1126/science.1207032

Cheng J, Ye L, Fu K, Wang H (2021) Effect of striker shape on impact energy absorption of a shear thickening fluid. Compos Commun 23:100560. https://doi.org/10.1016/j.coco.2020.100560

Egres RG, Wagner NJ (2005) The rheology and microstructure of acicular precipitated calcium carbonate colloidal suspensions through the shear thickening transition. J Rheol 49:719–746. https://doi.org/10.1122/1.1895800

Fu K, Wang H, Zhang YX et al (2020) Rheological and energy absorption characteristics of a concentrated shear thickening fluid at various temperatures. Int J Impact Eng 139:103525. https://doi.org/10.1016/j.ijimpeng.2020.103525

Gadkar A, Subramaniam KVL (2019) An evaluation of yield and Maxwell fluid behaviors of fly ash suspensions in alkali-silicate solutions. Mater Struct 52:117. https://doi.org/10.1617/s11527-019-1429-7

Guo F, Xu Z, Gu J (2023) Effects of nano-fumed silica and carbonyl iron powder of different particle sizes on the rheological properties of shear thickening fluids. Colloid Polym Sci 301:539–555. https://doi.org/10.1007/s00396-023-05087-0

Gürgen S, de Sousa RJA (2020) Rheological and deformation behavior of natural smart suspensions exhibiting shear thickening properties. Archiv Civ Mech Eng 20:110. https://doi.org/10.1007/s43452-020-00111-4

Heinze DA, Carastan DJ (2020) The influence of fumed silica content, dispersion energy, and humidity on the stability of shear thickening fluids. Rheol Acta 59:455–468. https://doi.org/10.1007/s00397-020-01216-6

Hu Y, Li K, Zhang B, Han B (2023) Effect of nano-SiO2 on mechanical properties, fluidity, and microstructure of superfine tailings cemented paste backfill. Mater Today Sustain 24:100490. https://doi.org/10.1016/j.mtsust.2023.100490

Jiang F, Pu W (2020) Salt induced shear thickening behavior of a hydrophobic association polymer and its potential in enhanced oil recovery. J Mater Sci 55:3130–3138. https://doi.org/10.1007/s10853-019-04221-0

Kanti P, Sharma KV, Ramachandra CG, Minea AA (2020) Effect of ball milling on the thermal conductivity and viscosity of Indian coal fly ash nanofluid. Heat Trans 49:4475–4490. https://doi.org/10.1002/htj.21836

Kim JH, Jun Y (2021) Decrease in viscosity caused by agglomeration and particle dispersion in cement–fly ash suspensions. Transp Res Rec 2675:73–80. https://doi.org/10.1177/03611981209406678

Li S, Wang J, Zhao S et al (2017) Giant rheological effect of shear thickening suspension comprising silica nanoparticles with no aggregation. J Mater Sci Technol 33:261–265. https://doi.org/10.1016/j.jmst.2016.06.008

Lin NYC, Guy BM, Hermes M et al (2015) Hydrodynamic and contact contributions to continuous shear thickening in colloidal suspensions. Phys Rev Lett 115:228304. https://doi.org/10.1103/PhysRevLett.115.228304

Liu M, Jiang W, Chen Q et al (2016) A facile one-step method to synthesize SiO_2@polydopamine core–shell nanospheres for shear thickening fluid. RSC Adv 6:29279–29287. https://doi.org/10.1039/C5RA25759J

Liu W, Li Y, Lin S et al (2020) Changes in chemical phases and microscopic characteristics of fly ash blended cement pastes in different CO2 concentrations. Constr Build Mater 257:119598. https://doi.org/10.1016/j.conbuildmat.2020.119598

Ma J, Wang D, Zhao S et al (2021) Influence of particle morphology of ground fly ash on the fluidity and strength of cement paste. Materials 14:283. https://doi.org/10.3390/ma14020283

Mahesh V, Harursampath D, Mahesh V (2022) An experimental study on ballistic impact response of jute reinforced polyethylene glycol and nano silica based shear thickening fluid composite. Def Technol 18:401–409. https://doi.org/10.1016/j.dt.2021.03.013

Mawkhlieng U, Majumdar A, Bhattacharjee D (2021) Graphene reinforced multiphase shear thickening fluid for augmenting low velocity ballistic resistance. Fibers Polym 22:213–221. https://doi.org/10.1007/s12221-021-0163-2

Monti A, Rosti ME (2023) Shear-thickening of dense bidispersed suspensions. Meccanica 58:727–737. https://doi.org/10.1007/s11012-023-01647-4

Nadziri N, Ismail I, Hamdan S (2018) Binding gel characterization of alkali-activated binders based on palm oil fuel ash (POFA) and fly ash. J Sustain Cement-Based Mater 7:1–14. https://doi.org/10.1080/21650373.2017.1299054

Prabhu TA, Singh A (2021) Effect of carrier fluid and particle size distribution on the rheology of shear thickening suspensions. Rheol Acta 60:107–118. https://doi.org/10.1007/s00397-021-01257-5

Qin J, Zhang G, Shi X (2016) Viscoelasticity of shear thickening fluid based on silica nanoparticles dispersing in 1-butyl-3-methylimidizolium tetrafluoroborate. J Dispers Sci Technol 37:1599–1606. https://doi.org/10.1080/01932691.2015.1125297

Rathee V, Arora S, Blair DL et al (2020) Role of particle orientational order during shear thickening in suspensions of colloidal rods. Phys Rev E 101:040601. https://doi.org/10.1103/PhysRevE.101.040601

Rizzo F, Pinto F, Meo M (2020) Investigation of silica-based shear thickening fluid in enhancing composite impact resistance. Appl Compos Mater 27:209–229. https://doi.org/10.1007/s10443-020-09805-7

Romagnoli M, Sassatelli P, Lassinantti Gualtieri M, Tari G (2014) Rheological characterization of fly ash-based suspensions. Constr Build Mater 65:526–534. https://doi.org/10.1016/j.conbuildmat.2014.04.130

Shen BH, Armstrong BL, Doucet M et al (2018) Shear thickening electrolyte built from sterically stabilized colloidal particles. ACS Appl Mater Interfaces 10:9424–9434. https://doi.org/10.1021/acsami.7b19441

Shi Y, Jiang K, Zhang T et al (2020) Clean production of porous-Al(OH)3 from fly ash. J Hazard Mater 393:122371. https://doi.org/10.1016/j.jhazmat.2020.122371

Siang Ng D, Paul SC, Anggraini V et al (2020) Influence of SiO2, TiO2 and Fe2O3 nanoparticles on the properties of fly ash blended cement mortars. Constr Build Mater 258:119627. https://doi.org/10.1016/j.conbuildmat.2020.119627

Son HS, Kim KH, Lee EH et al (2020) Enhanced shear thickening of silica colloidal suspension using polystyrene-polyacrylamide particles. Macromol Res 28:523–529. https://doi.org/10.1007/s13233-020-8069-1

Sun L, Zhu J, Wei M et al (2018) Effect of zirconia nanoparticles on the rheological properties of silica-based shear thickening fluid. Mater Res Express 5:055705. https://doi.org/10.1088/2053-1591/aac255

Sun L, Wang G, Zhang C et al (2021a) On the rheological properties of multi-walled carbon nano-polyvinylpyrrolidone/silicon-based shear thickening fluid. Nanotechnol Rev 10:1339–1348. https://doi.org/10.1515/ntrev-2021-0087

Sun L, Wei M, Zhu J (2021b) Low velocity impact performance of fiber-reinforced polymer impregnated with shear thickening fluid. Polym Testing 96:107095. https://doi.org/10.1016/j.polymertesting.2021.107095

Sun L, Liang T, Zhang C, Chen J (2023) The rheological performance of shear-thickening fluids based on carbon fiber and silica nanocomposite. Phys Fluids 35:032002. https://doi.org/10.1063/5.0138294

Sun L, Wang G, Zhang C (2024) Experimental investigation of a novel high performance multi-walled carbon nano-polyvinylpyrrolidone/silicon-based shear thickening fluid damper. J Intell Mater Syst Struct 35:661–672. https://doi.org/10.1177/1045389X231222999

Thiedeitz M, Kränkel T, Gehlen C (2022) Viscoelastoplastic classification of cementitious suspensions: transient and non-linear flow analysis in rotational and oscillatory shear flows. Rheol Acta 61:549–570. https://doi.org/10.1007/s00397-022-01358-9

Trulsson M, DeGiuli E, Wyart M (2017) Effect of friction on dense suspension flows of hard particles. Phys Rev E 95:012605. https://doi.org/10.1103/PhysRevE.95.012605

Wei M, Lv Y, Sun L, Sun H (2020) Rheological properties of multi-walled carbon nanotubes/silica shear thickening fluid suspensions. Colloid Polym Sci 298:243–250. https://doi.org/10.1007/s00396-020-04599-3

Wei M, Sun L, Gu W (2023) High strain rates impact performance of glass fiber-reinforced polymer impregnated with shear-thickening fluid. J Compos Sci 7:208. https://doi.org/10.3390/jcs7050208

Wilms P, Hinrichs J, Kohlus R (2022) Macroscopic rheology of non-Brownian suspensions at high shear rates: the influence of solid volume fraction and non-Newtonian behaviour of the liquid phase. Rheol Acta 61:123–138. https://doi.org/10.1007/s00397-021-01320-1

Wu Y, Cao S, Xuan S et al (2020) High performance zeolitic imidazolate framework-8 (ZIF-8) based suspension: improving the shear thickening effect by controlling the morphological particle-particle interaction. Adv Powder Technol 31:70–77. https://doi.org/10.1016/j.apt.2019.10.001

Yu M, Qiao X, Dong X, Sun K (2018) Effect of particle modification on the shear thickening behaviors of the suspensions of silica nanoparticles in PEG. Colloid Polym Sci 296:1767–1776. https://doi.org/10.1007/s00396-018-4399-3

Zheng B, Breton JR, Patel RS, Bhatia SR (2020) Microstructure, microrheology, and dynamics of laponite® and laponite®-poly(ethylene oxide) glasses and dispersions. Rheol Acta 59:387–397. https://doi.org/10.1007/s00397-020-01210-y

Zheng J, Liu Q, Wei W et al (2022) Roughness surface of raspberry-shaped silica nanoparticles effect on shear thickening colloidal suspensions. Appl Surf Sci 606:154917. https://doi.org/10.1016/j.apsusc.2022.154917